Azopyridinium-Containing [2]Pseudorotaxanes and Hydrazopyridinium-Containing [2]Catenanes[‡]

Peter R. Ashton,[a] Christopher L. Brown,[a] Jianguo Cao,[b] Ju-Young Lee,[a] Simon P. Newton,[a] Françisco M. Raymo,[b] J. Fraser Stoddart,*[b] Andrew J. P. White,[c] and David J. Williams*[c]

Keywords: Catenanes / Mechanically interlocked molecules / Molecular recognition / Pseudorotaxanes / Template synthesis

Benzylation of 4,4′-azopyridine, followed by counterion exchange, yields the bis(hexafluorophosphate) salt of the dibenzyl-4,4′-azopyridinium dication, which is bound by bis-*p*-phenylene-34-crown-10 (BPP34C10) and by 1,5-dioxynaphtho-38-crown-10 (1/5DN38C10) with K_a values of 90 and 880 M^{-1}, respectively, in acetonitrile. When a 4,4′-azopyridinium unit is introduced along with a bipyridinium unit into a tetracationic cyclophane — either in its free or catenated forms — spontaneous reduction to the 4,4′-hydrazopyridinium unit occurs. The X-ray structural analysis of a [2]catenane, incorporating this tetracationic cyclophane and BPP34C10, shows that the 4,4′-hydrazopyridinium unit is located alongside the cavity of the macrocyclic polyether while the other dicationic unit of the tetracationic cyclophane — namely the 4,4′-bipyridinium unit — is located inside. Variable temperature ^{1}H NMR spectroscopy demonstrated that the 4,4′-hydrazopyridinium unit rotates in solution around the [N···N] axis defined by its two pyridinium nitrogen atoms. The energy barrier for this dynamic process is ca. 14 kcal mol^{-1} in both the free tetracationic cyclophane and in the [2]catenane incorporating BPP34C10. However, the energy barrier for this dynamic process is only 11.7 kcal mol^{-1} in a [2]catenane incorporating the same tetracationic cyclophane and 1/5DN38C10. In this latter [2]catenane, the 4,4′-bipyridinium unit and the inside 1,5-dioxynaphthalene ring system rotate ($\Delta G_c^{\ddagger}$ 14.0 kcal mol^{-1}) in solution about their [N···N] and [O···O] axes, respectively. In the former [2]catenane, incorporating BPP34C10, the macrocyclic polyether circumrotates through the cavity of the tetracationic cyclophane against an energy barrier of 11.7 kcal mol^{-1}.

Introduction

The relative movements of the interlocked components of rotaxanes[1] and catenanes[1] can be exploited to perform switching operations at the molecular level.[2] The shuttling[3] of the macrocyclic component of a [2]rotaxane along the linear portion of its dumbbell-shaped component, and the circumrotation of one of the macrocyclic components of a [2]catenane through the cavity of the other, can be controlled[4,5] chemically, electrochemically, and/or photochemically by introducing appropriate units into one of the two interlocked components. We have developed[6] a template-directed synthetic strategy to construct [2]catenanes incorporating dioxyarene-based macrocyclic polyethers interlocked with cyclobis(paraquat-*p*-phenylene). This tetracationic cyclophane incorporates two 4,4′-bipyridinium units bridged by *p*-phenylene spacers. In its catenated form, one of the 4,4′-bipyridinium units is encircled by the macrocyclic polyether component while the other resides alongside it. In solution, the circumrotation of the tetracationic cyclophane through the cavity of the macrocyclic polyether exchanges the two 4,4′-bipyridinium units. By replacing one of the two 4,4′-bipyridinium units with an electrochemically and/or photochemically active unit, it should be possible to control this dynamic process reversibly by means of electrochemical and/or photochemical stimuli. Intrigued by this opportunity, we envisaged the possibility of replacing one of these 4,4′-bipyridinium units by a 4,4′-azopyridinium unit, and the incorporation of the resulting tetracationic cyclophane into [2]catenanes.[7] Here, we report: (i) the preparation of two 4,4′-azopyridinium-containing [2]pseudorotaxanes, (ii) the template-directed synthesis of one 4,4′-hydrazopyridinium-containing tetracationic cyclophane and of two [2]catenanes incorporating this tetracationic cyclophane as one of their interlocked components, (iii) the X-ray structural analyses of the linear component of the [2]pseudorotaxanes in its free form and of one [2]catenane, and (iv) the variable temperature ^{1}H NMR spectroscopic investigation of the tetracationic cyclophane and of the [2]catenanes.

[‡] Molecular Meccano, 62. − Part 61: P. R. Ashton, R. Ballardini, V. Balzani, A. Credi, R. Dress, E. Ishow, O. Kocian, J. A. Preece, N. Spencer, J. F. Stoddart, M. Venturi, S. Wenger, *Chem. Eur. J.* **2000**, *6*, 3558−3574.

[a] School of Chemistry, University of Birmingham, Edgbaston, Birmingham, B15 2TT, UK
[b] Department of Chemistry and Biochemistry, University of California, Los Angeles, 405 Hilgard Avenue, Los Angeles, CA 90095-1569, USA
Fax: (internat.) +1-310/206-1843
E-mail: stoddart@chem.ucla.edu
[c] Department of Chemistry, Imperial College, South Kensington, London, SW7 2AY, UK
Fax: (internat.) +44-207/594-5835

  1434−193X/01/0305−0957 $ 17.50+.50/0

Results and Discussion

Synthesis and Characterization

Treatment of 4-aminopyridine with an aqueous solution of NaOCl (Scheme 1) afforded 4,4′-azopyridine (**1**). Alkylation of **1** with $PhCH_2Br$, followed by counterion exchange, gave the 4,4′-azopyridinium-based compound **2**·$2PF_6$ in a yield of 82%. Initially, the liquid secondary ion mass spectrum (LSIMS) of **2**·$2PF_6$ revealed peaks at *m/z* values of 511 and 367 for $[M - PF_6]^+$ and $[M - 2PF_6]^+$, respectively, corresponding to the consecutive losses of the hexafluorophosphate counterions. It was noticed, however, that on further exposure to the primary Cs^+ ion beam there was a decrease in the intensity of the peak at *m/z* = 511 and the concomitant growth of a peak at *m/z* = 513. The high resolution analyses of the peaks at *m/z* = 511 and 513 confirmed elemental compositions of $C_{24}H_{22}F_6N_4P$ and $C_{24}H_{24}F_6N_4P$, respectively, suggesting that the 4,4′-azopyridinium unit of **2**·$2PF_6$ is reduced[8] to a 4,4′-hydrazopyridinium unit during the LSIMS analysis.

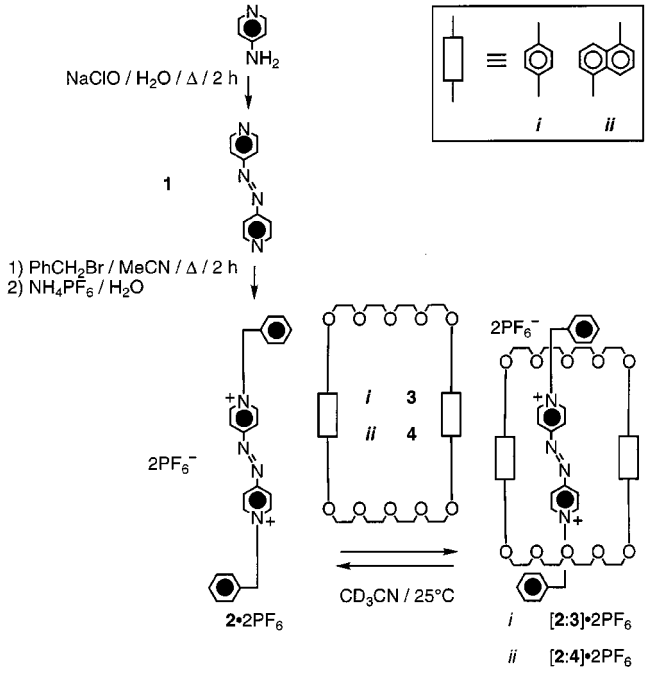

Scheme 1. The formation of the [2]pseudorotaxanes [**2**:**3**]·$4PF_6$ and [**2**:**4**]·$4PF_6$

When the π-electron deficient compound **2**·$2PF_6$ was combined (Scheme 1) with the π-electron rich macrocyclic polyether **3** (BPP34C10) or **4** (1/5DN38C10) in CD_3CN, the [2]pseudorotaxanes [**2**:**3**]·$2PF_6$ or [**2**:**4**]·$2PF_6$, respectively, formed spontaneously. The LSIMS of the [2]pseudorotaxanes revealed peaks at *m/z* values for $[M - PF_6]^+$ and $[M - 2PF_6]^+$ corresponding to the consecutive losses of the hexafluorophosphate counterions. The ^1H NMR spectrum (CD_3CN, 25 °C) of an equimolar solution of **2**·$2PF_6$ and **3** showed a significant chemical shift change ($\Delta\delta = -0.16$) for the set of signals associated with the β-pyridinium protons. When the macrocyclic polyether **4** was employed, the chemical shift change ($\Delta\delta = -0.39$) was even more pronounced. These observations indicate that the β-pyridinium protons of [**2**:**3**]·$2PF_6$ and [**2**:**4**]·$2PF_6$ suffer shielding effects exerted by the dioxyarene ring systems of the macrocyclic polyether components. The association constants (K_a) of [**2**:**3**]·$2PF_6$ and [**2**:**4**]·$2PF_6$ (K_a = 90 and 880 M^{-1}, respectively) were determined[9] by ^1H NMR spectroscopy (CD_3CN, 25 °C) using the dilution method. The K_a value increases by approximately one order of magnitude on replacing the two 1,4-dioxybenzene rings present in BPP34C10 (**3**) with 1,5-dioxynaphthalene ring systems to give 1/5DN38C10 (**4**). This enhancement of the K_a corresponds to an increase of the free energy of association ($-\Delta G°$) from 2.7 to 4.0 kcal mol^{-1}.

The reaction of 4,4′-azopyridine (**1**) with the bis(hexafluorophosphate) salt **5**·$2PF_6$, in the presence of the 1,5-dioxynaphthalene-based template **6**, gave[8] the 4,4′-hydrazopyridinium-containing tetracationic cyclophane **7**·$4PF_6$ in a yield of 22%, after counterion exchange (Scheme 2). The LSIMS of the tetracationic cyclophane revealed peaks at *m/z* values of 985, 839, and 694 for $[M - PF_6]^+$, $[M - 2PF_6]^+$, and $[M - 3PF_6]^+$, respectively, corresponding to the losses of the hexafluorophosphate counterions. The high resolution analysis of the peak at *m/z* = 985 indicated

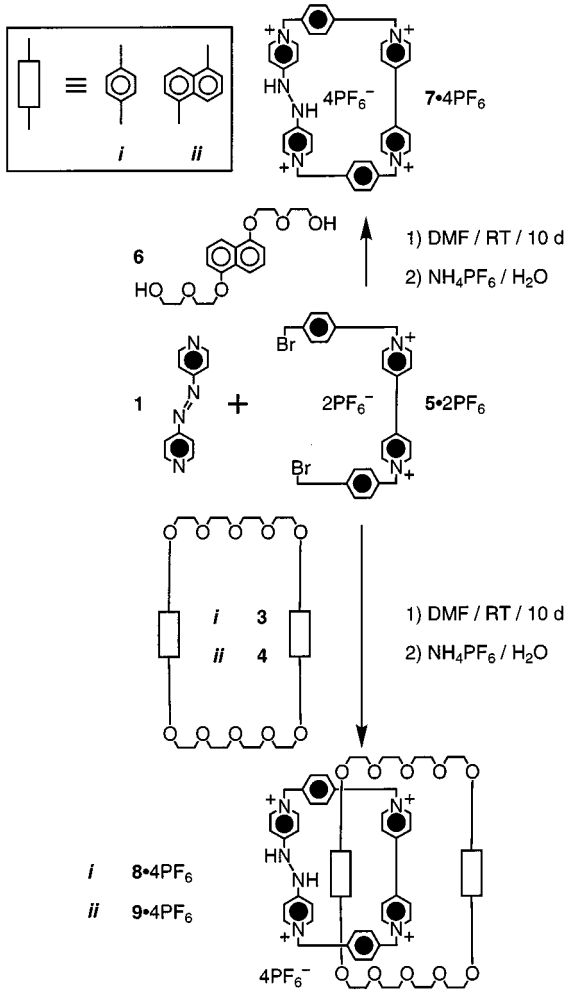

Scheme 2. The template-directed syntheses of the tetracationic cyclophane **7**·$4PF_6$ and of the [2]catenanes **8**·$4PF_6$ and **9**·$4PF_6$

an elemental composition of $C_{36}H_{34}F_{18}N_6O_{10}P_3$, confirming that this tetracationic cyclophane incorporates a 4,4′-hydrazopyridinium rather than a 4,4′-azopyridinium unit.

Reaction of 4,4′-azopyridine (**1**) with the bis(hexafluorophosphate) salt **5**·2PF_6, in the presence of BPP34C10 (**3**) or 1/5DN38C10 (**4**), gave[8] the 4,4′-hydrazopyridinium-containing [2]catenane **8**·4PF_6 or **9**·4PF_6 in yields of 40 or 68%, respectively, after counterion exchange (Scheme 2). The LSIMS of the [2]catenanes revealed peaks at *m*/*z* values for $[M - 2PF_6]^+$, $[M - 3PF_6]^+$, and $[M - 4PF_6]^+$ corresponding to the consecutive losses of the hexafluorophosphate counterions. The high resolution analyses of the peaks for $[M - 2PF_6]^+$ indicated elemental compositions of $C_{64}H_{73}F_{12}N_6O_{10}P_2$ and $C_{72}H_{77}F_{12}N_6O_{10}P_2$ for **8**·4PF_6 and **9**·4PF_6, respectively, confirming that the tetracationic cyclophane components of these [2]catenanes incorporate a 4,4′-hydrazopyridinium rather than a 4,4′-azopyridinium unit.

X-ray Crystallography

The X-ray analysis of the 4,4′-azopyridinium salt **2**·2PF_6 revealed the dication to have crystallographic C_2 symmetry about an axis passing through the central N=N double bond (Figure 1). The two pyridinium rings are almost coplanar with each other, the torsional twists about the N(1)−C(2) and N(1A)−C(2A) bonds being only ca. 4°. There is a small, but significant, rotation about the N=N double bond, the C(2)−N(1)−N(1A)−C(2A) torsion angle being 176.6(4)°. The double bond character of the N=N linkage is pronounced at 1.217(6) Å, although there is evidence for some delocalization into the N(1)−C(2) linkage which is slightly shorter at 1.446(4) Å than for a normal Ar−N single bond. The terminal benzyl groups are steeply inclined to their adjacent pyridinium ring systems, the torsional twists about the N(5)−C(8) and C(8)−C(14) bonds being ca. 22 and 87°, respectively. There are no intermolecular interactions of note.

Crystals of **8**·4PF_6 were obtained by vapor diffusion of PhH into a Me_2CO solution of the [2]catenane. A single crystal X-ray structural analysis (Figure 2) showed that only one of the two possible translational isomers is present in the solid state; this is the one incorporating the bipyridinium unit inside the cavity of the macrocyclic polyether. The [2]catenane has crystallographic C_2 symmetry about an axis passing through the center of the two 1,4-dioxybenzene rings and the bond linking the two pyridinium rings of the bipyridinium unit. Both 1,4-dioxybenzene rings are involved in an essentially symmetric π···π stacking interaction with the sandwiched bipyridinium unit (the mean planar separation is ca. 3.52 Å in each case). No significant C−H···O interactions were observed (the shortest H···O distance is 2.55 Å). Furthermore, the increased length of the 4,4′-hydrazopyridinium unit moves the two *p*-phenylene rings apart, weakening any potential C−H···π interaction between these rings and the 1,4-dioxybenzene hydrogen atoms (the shortest H···π distance is 3.24 Å). Further evidence for the lack of N=N double bond character in this compound is provided by the substantial torsional twist

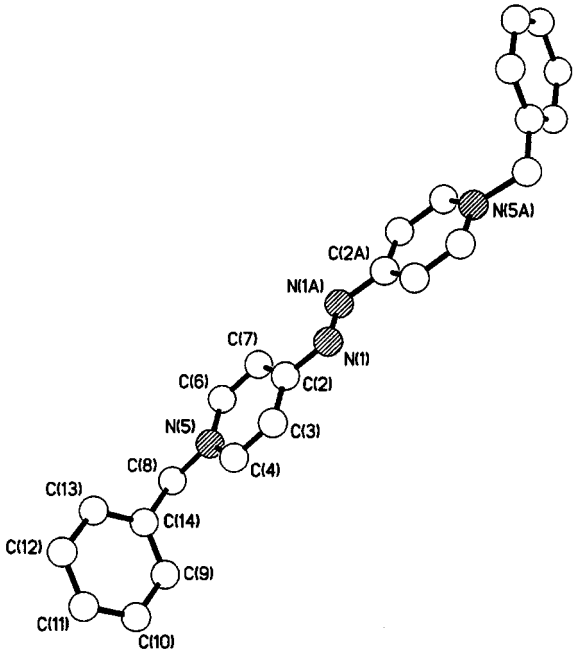

Figure 1. Ball-and-stick representation of the geometry adopted by the dication $\mathbf{2}^{2+}$ in the solid state

[127(1)°] about the N−N bond and by the associated bond length (1.36 Å) that is typical of a delocalized bond. Indeed, this bond is comparable with those between these nitrogen atoms and the carbon atoms of their adjacent pyridinium rings (1.36 Å). There is an absence of any intercatenane interactions and the packing is influenced by the presence of included PhH and Me_2CO molecules. The PhH molecules enter into mutual edge-to-face interactions, and one of them (and its C_2 symmetric counterpart) π-stacks with the hydrazopyridinium rings of the tetracation with a mean interplanar separation of 3.55 Å.

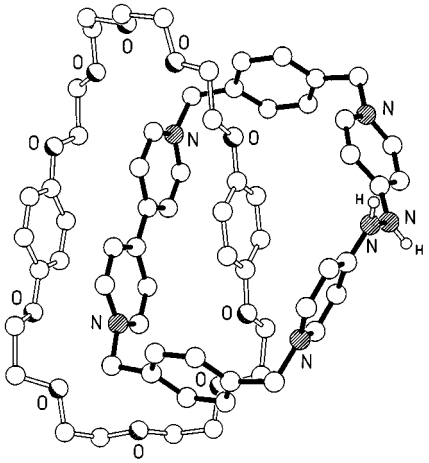

Figure 2. Ball-and-stick representation of the geometry adopted by the [2]catenane $\mathbf{8}^{4+}$ in the solid state

Variable Temperature ^{1}H NMR Spectroscopy

The local C_{2h} symmetry associated with the 4,4′-hydrazopyridinium unit of the tetracationic cyclophane **7**·4PF_6 imposes two sites (**A** and **B**) on the α-pyridinium protons H_α and H'_α and two sites (**C** and **D**) on the β-pyridinium pro-

tons H_β and H'_β (Figure 3). Exchange of the protons H_α and H'_α between the sites **A** and **B**, as well as of the protons H_β and H'_β between the sites **C** and **D**, occurs as a result of Process I. This dynamic process involves a 180° rotation of the pyridinium rings of the 4,4′-hydrazopyridinium unit around their [N···C4] axes. At 230 K in $(CD_3)_2CO$, Process I is slow on the ^1H NMR timescale and the protons H_α and H'_α give rise (Figure 4a) to two sets of signals (δ = 8.82 and 8.30). Similarly, two sets of resonances are observed for the protons H_β and H'_β (δ = 7.40 and 7.36), while the two protons of the hydrazo group give rise to a singlet (δ = 10.08). Upon warming the $(CD_3)_2CO$ solution of **7**·4PF_6, Process I becomes fast and the two sets of signals associated with the protons H_α and H'_α coalesce (Figure 4b and 4c) into one (δ = 8.57). Similarly, the two sets of resonances observed for the protons H_β and H'_β also coalesce into one (δ = 7.38). By employing the coalescence treatment, the energy barrier ($\Delta G_c^\ddagger$) for Process I was determined[10] (Table 1) using the protons H_α/H'_α and H_β/H'_β as probes.

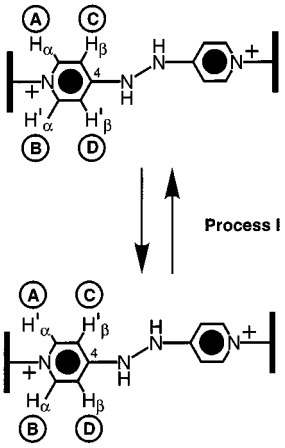

Figure 3. The 180° rotation (Process I) of the pyridinium rings of the 4,4′-hydrazopyridinium unit exchanging the protons H_α and H'_α between the sites **A** and **B** and the protons H_β and H'_β between the sites **C** and **D**

Comparison of the ^1H NMR spectrum of the tetracationic cyclophane **7**·4PF_6 with that of the [2]catenane **8**·4PF_6 revealed chemical shift changes of Δδ = −0.34 and −0.54 for the resonances associated with the α- and β-bipyridinium protons, respectively. These significant differences indicate that the macrocyclic polyether component of the [2]catenane encircles preferentially the bipyridinium unit, as observed (Figure 2) in the solid state. At 230 K in $(CD_3)_2CO$, Process I is also slow on the ^1H NMR timescale and the protons H_α and H'_α give rise to two sets of signals (δ = 8.77 and 8.13). Similarly, two sets of resonances are observed for the protons H_β and H'_β (δ = 7.19 and 6.60), while the two protons of the hydrazo group give rise to a singlet (δ = 10.07). Upon warming the $(CD_3)_2CO$ solution of **8**·4PF_6, Process I becomes fast and the two sets of signals associated with the protons H_α and H'_α coalesce into one (δ = 8.34). Similarly, the two sets of resonances observed for the protons H_β and H'_β also coalesce into one (δ = 6.90). By employing the coalescence treatment, the $\Delta G_c^\ddagger$ value for Process I was determined[10] using the protons H_α/H'_α and H_β/H'_β as probes (Table 1). Interestingly, no significant difference was observed between the $\Delta G_c^\ddagger$ value associated with the tetracationic cyclophane **7**·4PF_6 and that for the [2]catenane **8**·4PF_6. The 1,4-dioxybenzene rings located inside and alongside the cavity of the tetracationic cyclophane component of the [2]catenane **8**·4PF_6 are exchanged (Figure 5) as a result of Process II. This dynamic process involves the circumrotation of the macrocyclic polyether through the cavity of the tetracationic cyclophane. At 230 K in $(CD_3)_2CO$, Process I is slow on the ^1H NMR timescale and the protons H_{db} and H'_{db} give rise (Figure 6a) to two distinct signals (δ = 6.22 and 4.60). Upon warming the $(CD_3)_2CO$ solution of **8**·4PF_6 up, Process II becomes fast and the two signals associated with the protons H_{db} and H'_{db} coalesce (Figure 6b and 6c) into one (δ = 5.48). By employing the coalescence treatment, the $\Delta G_c^\ddagger$ value for Process II was determined[10] using the protons H_{db}/H'_{db} as probes (Table 1).

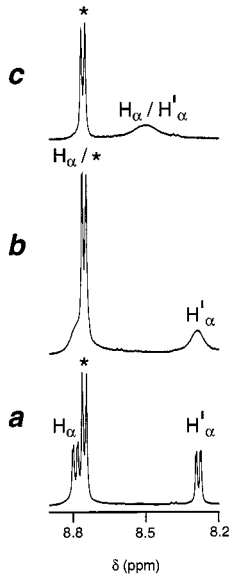

Figure 4. Partial ^1H NMR spectra of the tetracationic cyclophane **7**·4PF_6 recorded in $(CD_3)_2CO$ at (***a***) 230, (***b***) 280, and (***c***) 320 K (the set of signals labeled with the symbol * corresponds to the β-bipyridinium protons)

Table 1. Kinetic parameters (determined by variable temperature ^1H NMR spectroscopy at 400 MHz) for the dynamic processes associated with the tetracationic cyclophane **7**·4PF_6 and with the [2]catenanes **8**·4PF_6 and **9**·4PF_6 in $(CD_3)_2CO$

Compound	Probe Protons	Δν≅[a] (Hz)	k_c[b] (s^{-1})	T_c[c] (K)	$\Delta G_c^\ddagger$ [d] (kcal mol^{-1})	Process
7·4PF_6	H_α/H'_α	203	450	304	14.1	I
	H_β/H'_β	37	83	288	14.5	I
8·4PF_6	H_α/H'_α	262	582	304	14.0	I
	H_β/H'_β	246	546	304	14.0	I
	H_{db}/H'_{db}	648	1440	280	12.3	II
9·4PF_6	H_α/H'_α	54	119	240	11.7	I
	H_{bp}/H'_{bp}	80	177	291	14.0	III/IV

[a] Limiting frequency separation (error = ± 1 Hz). − [b] Rate constant at the coalescence temperature (error = ± 5 Hz). − [c] Coalescence temperature (error = ± 1 K). − [d] Free energy barrier at the coalescence temperature (error = ± 0.2 kcal mol^{-1}).

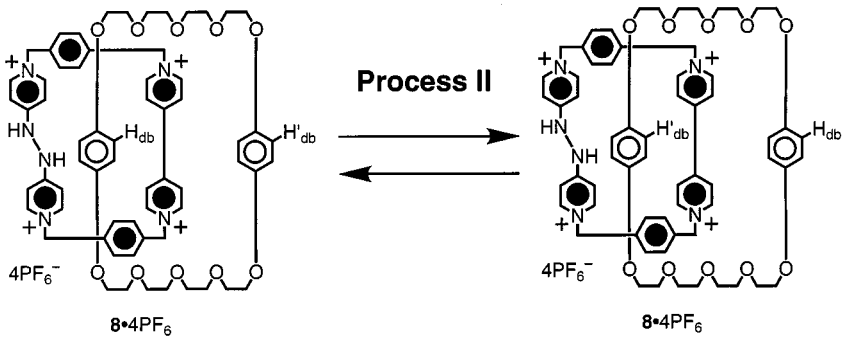

Figure 5. The circumrotation (Process II) of the macrocyclic polyether through the cavity of the tetracationic cyclophane component of the [2]catenane **8**·4PF$_6$ exchanging the "inside" and "alongside" 1,4-dioxybenzene protons H_{db} and H'_{db}

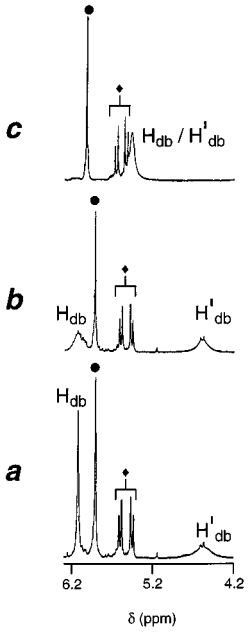

Figure 6. Partial ^{1}H NMR spectra of the [2]catenane **8**·4PF$_6$ recorded in $(CD_3)_2CO$ at (***a***) 230, (***b***) 260, and (***c***) 320 K (the signals labeled with the symbols and ◆ correspond to the protons of the methylene groups adjacent to the 4,4′-bipyridinium and 4,4′-hydrazopyridinium units, respectively)

Comparison of the ^{1}H NMR spectrum of the tetracationic cyclophane **7**·4PF$_6$ with that of the [2]catenane **9**·4PF$_6$ revealed chemical shift changes of $\Delta\delta = -0.63$ and -1.49 for the resonances associated with the α- and β-bipyridinium protons, respectively. These significant differences indicate that the macrocyclic polyether component of the [2]catenane encircles preferentially the bipyridinium unit, as observed for the [2]catenane **8**·4PF$_6$. At 205 K in $(CD_3)_2CO$, Process I is also slow and the protons H_α and H'_α give rise to two sets of signals ($\delta = 8.21$ and 8.11). Upon warming the $(CD_3)_2CO$ solution of **9**·4PF$_6$, Process I becomes fast and these two sets of signals coalesce into one ($\delta = 8.16$). By employing the coalescence treatment, the $\Delta G_c^\ddagger$ value for Process I was determined[10] using the protons H_α/H'_α as probes (Table 1). Interestingly, in the case of the [2]catenane **9**·4PF$_6$ the $\Delta G_c^\ddagger$ value for Process I is ca. 2 kcal mol^{-1} lower than those associated with the tetracationic cyclophane **7**·4PF$_6$ and the [2]catenane **8**·4PF$_6$.

The local C_{2h} symmetry associated with the 1,5-dioxynaphthalene ring system located inside the cavity of tetracationic cyclophane imposes two sites (**E** and **F**) on the α-bipyridinium protons H_{bp} and H'_{bp} (Figure 7). Exchange of these protons between the sites **E** and **F** occurs as a result of Process III and/or Process IV. Process III involves: (i) the dislodgment of the 1,5-dioxynaphthalene ring system from the cavity of the tetracationic cyclophane, (ii) its 180° rotation about its [O···O] axis, and (iii) its reinsertion inside the cavity of the tetracationic cyclophane. Process IV involves:

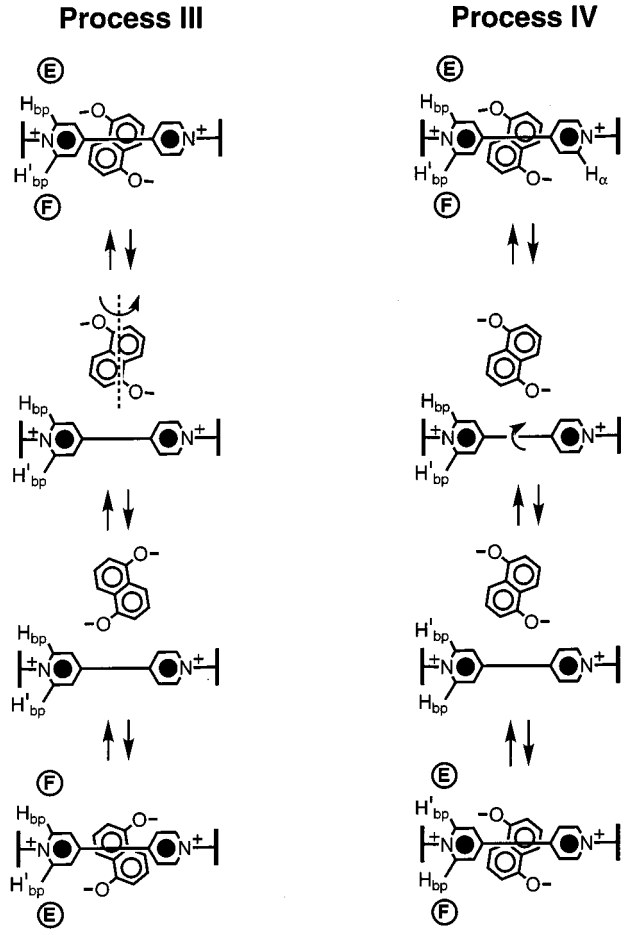

Figure 7. The dynamic processes (Process III and Process IV) associated with the [2]catenane exchanging the α-bipyridinium protons H_{bp} and H'_{bp} between the sites E and F

(i) the dislodgment of the 1,5-dioxynaphthalene ring system from the cavity of the tetracationic cyclophane, (ii) the 180° rotation of the 4,4′-bipyridinium unit about its [N···N] axis, and (iii) the reinsertion of the 1,5-dioxynaphthalene ring system inside the cavity of the tetracationic cyclophane. At 230 K in $(CD_3)_2CO$, Process III and Process IV are slow and the protons H_{bp} and H'_{bp} give rise to two sets of signals (δ = 9.25 and 8.80) (Figure 8a). Upon warming the $(CD_3)_2CO$ solution of **9**·4PF_6 up, Process III and/or Process IV become fast and these two sets of signals coalesce (Figure 8b and Figure 8c) into one (δ = 8.98). By employing the coalescence treatment, the $\Delta G_c^{\ddagger}$ for Process III or Process IV, or a combination of both, was determined[10] (Table 1) using the protons H_{bp} and H'_{bp} as probes.

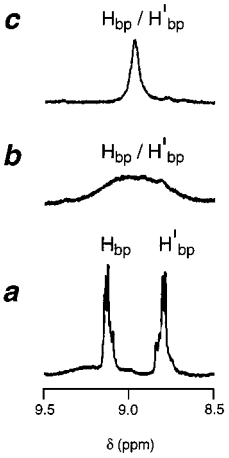

Figure 8. Partial ^1H NMR spectra of the [2]catenane **9**·4PF_6 recorded in $(CD_3)_2CO$ at (***a***) 230, (***b***) 290, and (***c***) 320 K

Conclusions

In acetonitrile, BPP34C10 and 1/5DN38C10 bind (with K_a values of 90 and 880 M^{-1}, respectively) a 4,4′-azopyridinium-containing guest inside their π-electron rich cavities. When 1,5-dioxynaphthalene ring systems, rather than 1,4-dioxybenzene rings, are incorporated in the host, a significantly more stable complex is obtained. Upon introduction of a 4,4′-azopyridinium unit into a tetracationic cyclophane, this unit is reduced unexpectedly to a 4,4′-hydrazopyridinium unit. Even when this tetracationic cyclophane is interlocked with BPP34C10 or with 1/5DN38C10, reduction occurs spontaneously. Of the two possible translational isomers associated with each [2]catenane, only one is observed in solution and in the solid state. In both [2]catenanes, the 4,4′-hydrazopyridinium unit resides alongside the cavity of the macrocyclic polyether while the other π-electron deficient unit incorporated within the tetracationic cyclophane is located inside. In solution, the 4,4′-hydrazopyridinium of the free and of the catenated tetracationic cyclophane rotates about the [N···N] axis defined by its two pyridinium nitrogen atoms. In the [2]catenane incorporating 1/5DN38C10, the energy barrier associated with this dynamic process is ca. 2 kcal mol^{-1} lower than that for the other [2]catenane and that for the free tetracationic cyclophane. The 4,4′-bipyridinium unit and the inside 1,5-dioxynaphthalene ring systems of the [2]catenane incorporating 1/5DN38C10 also rotate ($\Delta G_c^{\ddagger}$ = 14.0 kcal mol^{-1}) around their [N···N] and [O···O] axes, respectively. In the other [2]catenane, the macrocyclic polyether circumrotates ($\Delta G_c^{\ddagger}$ = 11.7 kcal mol^{-1}) through the cavity of the tetracationic cyclophane component.

Although we have been thwarted in our bid to self-assemble a photochemically switchable [2]catenane by the apparently unavoidable spontaneous reduction of the 4,4′-azopyridinium unit in the "asymmetric" tetracationic cyclophane interlocked with either BPP34C10 or 1/5DN38C10, we recall that, although [2]catenanes[11] in which either BPP34C10 or 1/5DN38C10 is encircled by a tetracationic cyclophane containing one bipyridinium and one bis(pyridinium)ethylene unit cannot be switched photochemically, they can be switched electrochemically. In view of our recent success[12] in being able to incorporate an electrochemically switchable [2]catenane — in which cyclobis(paraquat-*p*-phenylene) is encircled by a crown ether containing one tetrathiafulvalene unit and one 1,5-dioxynaphthalene ring system — into a solid-state electronically reconfigurable switching device, we intend to re-examine the switchable [2]catenanes in which the π-electron accepting groups in the tetracationic cyclophane are different and can be addressed electrochemically in such a manner that circumrotation of the tetracationic cyclophane through the crown ether macrocycle can be redox activated between two mechanically different states.

Experimental Section

General Methods: Chemicals were purchased from Aldrich and used as received. Solvents were dried according to literature procedures.[13] The compounds **3**,[14] **4**,[15] and **5**·2PF_6 [16] were prepared as described previously in the literature. − Thin layer chromatography (TLC) was carried out on aluminum sheets coated with silica-gel 60 (Merck 5554). Column chromatography was performed on silica-gel 60 (Merck 9385, 230−400 mesh). − Melting points were determined on an Electrothermal 9200 melting point apparatus and are uncorrected. − Electron impact mass spectra (EIMS) were recorded on a Kratos Profile spectrometer. Liquid secondary ion mass spectra (LSIMS) were recorded on a VG Zabspec spectrometer, equipped with a Cs^+ source, using 3-nitrobenzyl alcohol as matrix. For high resolution LSIMS (HRLSIMS), the instrument was operated at a resolution of ca. 6000 by employing narrow range voltage scanning along with polyethylene glycol or CsI as reference compounds. Electrospray mass spectra (ESMS) were recorded on a Micromass LCT spectrometer using MeOH as mobile phase. − ^1H and ^{13}C NMR spectra were recorded on a Bruker ARX400 (400 and 100.6 MHz, respectively) spectrometer. − Elemental analyses were performed by Quantitative Technologies Inc.

4,4′-Azopyridinium (1): An aqueous solution of NaOCl (12−13%, 200 mL) was added dropwise to a solution of 4-aminopyridine (5 g, 53 mmol) in H_2O (40 mL). The mixture was heated under reflux for 2 h. After cooling to ambient temperature, the solution was extracted with Et_2O (3 × 100 mL). The organic phase was concentrated under reduced pressure and the residue was purified by column chromatography (SiO_2, $MeCO_2Et$) to afford **1** (0.7 g, 8%) as a red solid. − M.p. 106−108 °C (ref.[17] 108−109 °C). − EIMS:

m/z = 184 $[M]^+$. − ^{1}H NMR ($CDCl_3$): δ = 8.66 (d, *J* = 6 Hz, 4 H), 7.53 (d, *J* = 6 Hz, 4 H). − ^{13}C NMR ($CDCl_3$): δ = 155.9, 151.2, 115.9. − $C_{10}H_8N_4$ (184.202): calcd. C 65.22, H 4.35, N 30.43; found C 64.09, H 4.10, N 29.74.

1,1′-Bisbenzyl-4,4′-azopyridinium Bis(hexafluorophosphate) (2·2PF$_6$): A solution of **1** (50 mg, 0.27 mmol) and $PhCH_2Br$ (93 mg, 0.54 mmol) in MeCN (100 mL) was heated to reflux under an atmosphere of N_2 for 3 h. After cooling to ambient temperature, the precipitate was filtered off, washed with MeCN and Et_2O, and dissolved in H_2O (10 mL). After the addition of NH_4PF_6, **3**·2PF$_6$ (146 mg, 82%) precipitated out as a red solid. − M.p. >250 °C. − LSIMS: *m/z* = 511 $[M - PF_6]^+$, 367 $[M - 2PF_6]^+$. − HRLSIMS: *m/z* calcd. for $[M - PF_6]^+$ ($C_{24}H_{22}F_6N_4P$): 511.1486; found 511.1479. − ESMS: *m/z* = 679 $[M + Na]^+$, 511 $[M - PF_6]^+$, 367 $[M - 2PF_6]^+$. − ^{1}H NMR (CD_3CN): δ = 9.00 (d, *J* = 6 Hz, 4 H), 8.34 (d, *J* = 6 Hz, 4 H), 7.51 (s, 10 H), 5.82 (s, 4 H). − ^{13}C NMR (CD_3CN): δ = 137.5, 135.4, 134.8, 134.7, 126.6, 122.5, 70.1. − $C_{24}H_{22}F_{12}N_4P_2$ (656.392): calcd. C 43.90, H 3.35, N 8.54; found C 43.69, H 3.25, N 8.36.

Crystal data: $[C_{24}H_{22}N_4][PF_6]_2$, *M* = 656.4, monoclinic, space group *C*2/*c* (no. 15), *a* = 19.359(1), *b* = 8.204(1), *c* = 18.932(1) Å, β = 113.32(1)°, *V* = 2760.8(3) Å^3, *Z* = 4 (the molecule has crystallographic C_2 symmetry), D_c = 1.579 g cm^{-3}, μ(Cu-K_α) = 24.1 cm^{-1}, *F*(000) = 1328, *T* = 293 K; orange/red platy rhombs, 0.83 × 0.50 × 0.17 mm, Siemens P4/PC diffractometer, ω-scans, 2173 independent reflections. The structure was solved by direct methods and the non-hydrogen atoms were refined anisotropically using full matrix least-squares based on F^2 to give R_1 = 0.078, wR_2 = 0.224 for 1721 independent observed reflections [$|F_o| > 4\sigma(|F_o|)$, 2θ ≤ 124°] and 179 parameters.

Crystallographic data (excluding structure factors) for this structure have been deposited with the Cambridge Crystallographic Data Centre as supplementary publication no. CCDC-154037. Copies of the data can be obtained free of charge on application to CCDC, 12 Union Road, Cambridge CB2 1EZ, UK [Fax: (internat.) + 44-1223/336-033; Email: deposit@ccdc.cam.ac.uk].

[2]-[(Bis-*p*-phenylene-34-crown-10)-(1,1′-Bisbenzyl-4,4′-hydrazopyridinium)]pseudorotaxane Bis(hexafluorophosphate) ([2:3]·2PF$_6$) and [2]-[(1,5-Dinaphtho-38-crown-10)-(1,1′-Bisbenzyl-4,4′-azopyridinium)]pseudorotaxane Bis(hexafluorophosphate) ([2:4]·2PF$_6$): A solution of **2**·2PF$_6$ (6.6 mg, 0.01 mmol) in CD_3CN (1 mL) was mixed with a solution of either **3** (5.4 mg, 0.01 mmol) or **4** (6.4 mg, 0.01 mmol) to afford [**2**:**3**]·2PF$_6$ or [**2**:**4**]·2PF$_6$, respectively.

[**2**:**3**]·2PF$_6$: K_a = 90 M^{-1}, Δ*G*° = −2.7 kcal mol^{-1}, *T* = 25 °C. − LSIMS: *m/z* = 1050 $[M - PF_6]^+$, 904 $[M - 2PF_6]^+$. − ^{1}H NMR (CD_3CN): δ = 9.06 (d, *J* = 7 Hz, 4 H), 8.18 (d, *J* = 7 Hz, 4 H), 7.55−7.50 (m, 10 H), 6.45 (s, 8 H), 5.83 (s, 4 H), 3.58−3.71 (m, 32 H).

[**2**:**4**]·2PF$_6$: K_a = 880 M^{-1}, Δ*G*° = −4.0 kcal mol^{-1}, *T* = 25 °C. − LSIMS: *m/z* = 1150 $[M - PF_6]^+$, 1004 $[M - 2PF_6]^+$. − ^{1}H NMR (CD_3CN): δ = 9.00 (d, *J* = 7 Hz, 4 H), 7.95 (d, *J* = 7 Hz, 4 H), 7.59−7.51 (m, 10 H), 7.37 (d, *J* = 9 Hz), 4 H, 7.05 (pt, *J* = 9 Hz, 4 H), 6.42 (d, *J* = 9 Hz, 4 H), 5.84 (s, 4 H), 3.84−3.70 (m, 32 H).

Cyclo(paraquat-*p*-phenylene-4,4′-hydrazobipyridinium-*p*-phenylene) Tetrakis(hexafluorophosphate) (7·4PF$_6$): A solution of **1** (66 mg, 0.36 mmol), **5**·2PF$_6$ (450 mg, 0.54 mmol), and **6** (363 mg, 1.08 mmol) in DMF (5 mL) was stirred for 10 days at ambient temperature. The solvent was distilled under reduced pressure and the residue was purified by column chromatography (SiO_2, MeOH/2 M NH_4Cl_{aq}/$MeNO_2$, 7:2:1) to afford a product which was dissolved in H_2O. After the addition of NH_4PF_6, **7**·4PF$_6$ (90 mg, 22%) precipitated out as a white solid. − M.p. >250 °C. − LSIMS: *m/z* = 985 $[M - PF_6]^+$, 839 $[M - 2PF_6]^+$, 694 $[M - 3PF_6]^+$. − HRLSIMS: *m/z* calcd. for $[M - PF_6]^+$ ($C_{36}H_{34}F_{18}N_6O_{10}P_3$): 985.1770; found 985.1799. − ESMS: *m/z* = 839 $[M - 2PF_6]^+$, 694 $[M - 3PF_6]^+$. − ^{1}H NMR [$(CD_3)_2CO$, 230 K]: δ = 10.08 (s, 2 H), 9.60 (d, *J* = 7 Hz, 4 H), 8.82 (d, *J* = 6 Hz, 2 H), 8.77 (d, *J* = 7 Hz, 4 H), 8.30 (d, *J* = 7 Hz, 2 H), 7.80 (d, *J* = 8 Hz, 4 H), 7.64 (d, *J* = 8 Hz, 4 H), 7.40 (d, *J* = 6 Hz, 2 H), 7.36 (d, *J* = 6 Hz, 2 H), 6.17 (s, 4 H), 5.70 (d, *J* = 14 Hz, 2 H), 5.56 (d, *J* = 14 Hz, 2 H). − ^{13}C NMR [$(CD_3)_2CO$, 300 K]: δ = 158.8, 150.3, 146.2, 144.6, 136.5, 136.3, 130.9, 130.5, 128.8, 128.2, 65.2, 61.8.

[2]-{(Bis-*p*-phenylene-34-crown-10)-[cyclo(paraquat-*p*-phenylene-4,4′-hydrazobipyridinium-*p*-phenylene)]}catenane Tetrakis(hexafluorophosphate) (8·4PF$_6$) and [2]-{(1,5-Dinaphtho-38-crown-10)-[cyclo(paraquat-*p*-phenylene-4,4′-hydrazobipyridinium-*p*-phenylaene)]}catenane Tetrakis(hexafluorophosphate) (9·4PF$_6$): A solution of **1** (51 mg, 0.28 mmol), **5**·2PF$_6$ (227 mg, 0.28 mmol), and either **3** (50 mg, 0.09 mmol) or **4** (64 mg, 0.09 mmol) in DMF (5 mL) was stirred for 10 days at ambient temperature. The solvent was distilled off under reduced pressure and the residue was purified by column chromatography (SiO_2, MeOH/2 M NH_4Cl_{aq}/$MeNO_2$, 7:2:1) to afford a product which was dissolved in H_2O. After the addition of NH_4PF_6, **8**·4PF$_6$ or **9**·4PF$_6$ precipitated out as a red or purple solid, respectively.

8·4PF$_6$ (62 mg, 40%): M.p. > 250 °C. − LSIMS: *m/z* = 1375 $[M - 2PF_6]^+$, 1230 $[M - 3PF_6]^+$, 1085 $[M - 4PF_6]^+$. − HRLSIMS: *m/z* calcd. for $[M - 2PF_6]^+$ ($C_{64}H_{74}F_{12}N_6O_{10}P_2$): 1375.4672; found 1375.4701. − ESMS: *m/z* = 1543 $[M - PF_6 + Na]^+$, 1375 $[M - 2PF_6]^+$, 1230 $[M - 3PF_6]^{2+}$. − ^{1}H NMR [$(CD_3)_2CO$, 230 K]: δ = 10.07 (s, 2 H), 9.26 (br s, 4 H), 8.77 (d, *J* = 7 Hz, 2 H), 8.23 (br s, 4 H), 8.13 (d, *J* = 7 Hz, 2 H), 8.02 (d, *J* = 8 Hz, 4 H), 7.83 (d, *J* = 8 Hz, 4 H), 7.19 (br s, 2 H), 6.60 (br s, 2 H), 6.22 (s, 4 H), 6.00 (s, 4 H), 5.69 (d, *J* = 14 Hz, 2 H), 5.53 (d, *J* = 14 Hz, 2 H), 4.60 (br s, 4 H), 3.93−3.60 (m, 32 H). − ^{13}C NMR [$(CD_3)_2CO$, 230 K]: δ = 157.8, 152.5, 151.3, 146.2, 137.2, 136.8, 131.6, 131.3, 125.8, 115.3, 71.0, 70.6, 70.1.

Crystals suitable for X-ray structural analysis were obtained by vapor diffusion of C_6H_6 into a Me_2CO solution of the [2]catenane. Crystal data: $[C_{64}H_{74}N_6O_{10}][PF_6]_4$·3PhH·3$Me_2CO$·$H_2O$, *M* = 2093.8, monoclinic, space group *C*2/*c* (no. 15), *a* = 30.903(13), *b* = 18.569(4), *c* = 21.436(11) Å, β = 115.20(4)°, *V* = 11130(8) Å^3, *Z* = 4 (the molecule has crystallographic C_2 symmetry), D_c = 1.249 g cm^{-3}, μ(Cu-K_α) = 14.7 cm^{-1}, *F*(000) = 4352, *T* = 213 K; red blocks, 0.67 × 0.53 × 0.53 mm, Siemens P4/RA diffractometer, ω-scans, 8076 independent reflections. The structure was solved by direct methods and the non-hydrogen atoms were refined anisotropically using full matrix least-squares based on F^2 to give R_1 = 0.127, wR_2 = 0.357 for 5052 independent observed reflections [$|F_o| > 4\sigma(|F_o|)$, 2θ ≤ 120°] and 653 parameters.

Crystallographic data (excluding structure factors) for this structure have been deposited with the Cambridge Crystallographic Data Centre as supplementary publication no. CCDC-154036. Copies of the data can be obtained free of charge on application to CCDC, 12 Union Road, Cambridge CB2 1EZ, UK [Fax: (internat.) + 44-1223/336-033; Email: deposit@ccdc.cam.ac.uk].

9·4PF$_6$ (120 mg, 68%): M.p. 188−190 °C. − LSIMS: *m/z* = 1476 $[M - 2PF_6]^+$, 1331 $[M - 3PF_6]^+$, 1185 $[M - 4PF_6]^+$. − HRLSIMS: *m/z* calcd. for $[M - 2PF_6]^+$ ($C_{72}H_{78}F_{12}N_6O_{10}P_2$): 1475.4985; found 1475.4997. − ESMS: *m/z* = 1643 $[M + Na - PF_6]^+$, 1476 $[M - 2PF_6]^+$, 1331 $[M - 3PF_6]^+$, 1186 $[M - 4PF_6]^+$. − ^{1}H NMR (CD_3CN, 320 K): δ = 9.09 (br, s 4 H), 8.94−8.92 (m, 4 H), 7.95 (s, 8 H), 7.30 (br, s, 4 H), 7.20 (d, *J* = 8 Hz, 2 H), 7.11 (pt, *J* = 8 Hz, 2 H), 6.84 (br, s, 4 H) 6.35 (d, *J* = 8 Hz, 2 H), 6.14 (d, *J* = 8 Hz, 2 H), 5.87−5.84 (m, 6 H), 5.65 (d, *J* = 8 Hz, 2 H),

5.50 (pt, J = 8 Hz, 2 H), 4.07−3.69 (m, 32 H), 3.08 (d, J = 8 Hz, 2 H). − ^{13}C NMR [$(CD_3)_2CO$, 300 K]: δ = 155.2, 143.8, 138.4, 136.2, 131.6, 131.2, 126.3, 71.9, 71.7, 70.8, 68.2, 65.3, 61.6.

Acknowledgments

This research was supported at the University of Birmingham by EPSRC and at UCLA by DARPA.

[1] For accounts, books, and reviews on catenanes and rotaxanes, see: [1a] G. Schill, *Catenanes, Rotaxanes and Knots*, Academic Press, New York, **1971**. − [1b] D. M. Walba, *Tetrahedron* **1985**, *41*, 3161−3212. − [1c] C. O. Dietrich-Buchecker, J.-P. Sauvage, *Chem. Rev.* **1987**, *87*, 795−810. − [1d] Y. S. Lipatov, T. E. Lipatova, L. F. Kosyanchuk, *Adv. Polym. Sci.* **1989**, *88*, 49−76. − [1e] J.-P. Sauvage, *Acc. Chem. Res.* **1990**, *23*, 319−327. − [1f] C. O. Dietrich-Buchecker, J.-P. Sauvage, *Bioorg. Chem. Front.* **1991**, *2*, 195−248. − [1g] H. W. Gibson, H. Marand, *Adv. Mater.* **1993**, *5*, 11−21. − [1h] J.-C. Chambron, C. O. Dietrich-Buchecker, J.-P. Sauvage, *Top. Curr. Chem.* **1993**, *165*, 131−162. − [1i] F. Bickelhaupt, *J. Organomet. Chem.* **1994**, *475*, 1−14. − [1j] H. W. Gibson, M. C. Bheda, P. T. Engen., *Prog. Polym. Sci.* **1994**, *19*, 843−945. − [1k] D. B. Amabilino, I. W. Parsons, J. F. Stoddart, *Trends Polym. Sci.* **1994**, *2*, 146−152. − [1l] D. B. Amabilino, J. F. Stoddart, *Chem. Rev.* **1995**, *95*, 2725−2828. − [1m] F. Vögtle, T. Dünnwald, T. Schmidt, *Acc. Chem. Res.* **1996**, *29*, 451−460. − [1n] A. C. Benniston, *Chem. Soc. Rev.* **1996**, *25*, 427−435. − [1o] M. Fujita, K. Ogura, *Coord. Chem. Rev.* **1996**, *148*, 249−264. − [1p] M. Belohradsky, F. M. Raymo, J. F. Stoddart, *Collect. Czech. Chem. Commun.* **1996**, *61*, 1−43. − [1q] F. M. Raymo, J. F. Stoddart, *Trends Polym. Sci.* **1996**, *4*, 208−211. − [1r] R. Jäger R., F. Vögtle, *Angew. Chem. Int. Ed. Engl.* **1997**, *36*, 930−944. − [1s] M. Belohradsky, F. M. Raymo, J. F. Stoddart, *Collect. Czech. Chem. Commun.* **1997**, *62*, 527−557. − [1t] S. A. Nepogodiev, J. F. Stoddart, *Chem. Rev.* **1998**, *98*, 1959−1976. − [1u] J.-C. Chambron, J.-P. Sauvage, *Chem. Eur. J.* **1998**, *4*, 1362−1366. − [1v] S. A. Nepogodiev, J. F. Stoddart, *Chem. Rev.* **1998**, *98*, 1959−1976. − [1w] M. Fujita, *Acc. Chem. Res.* **1999**, *32*, 53−61. − [1x]*Molecular Catenanes, Rotaxanes and Knots* (Eds.: C. O. Dietrich-Buckecher, J.-P. Sauvage), Wiley-VCH, Weinheim, **1999**. − [1y]G. A. Breault, C. A. Hunter, P. C. Mayers, *Tetrahedron* **1999**, *55*, 5265−5293. − [1z] F. M. Raymo, J. F. Stoddart, *Chem. Rev.* **1999**, *99*, 1643−1664.

[2] For accounts and reviews on molecular and supramolecular switches, see: [2a] V. Balzani, F. Scandola, *Supramolecular Photochemistry*, Horwood, Chichester, **1991**. − [2b] V. Balzani, *Tetrahedron* **1992**, *48*, 10443−10514. − [2c] R. A. Bissell, A. P. de Silva, H. Q. N. Gunaratne, P. L. M. Lynch, G. E. M. Maguire, K. R. A. S. Sandanayake, *Chem. Soc. Rev.* **1992**, *21*, 187−195. − [2d] R. A. Bissell, A. P. de Silva, H. Q. N. Gunaratne, P. L. M. Lynch, G. E. M. Maguire, C. P. McCoy, K. R. A. S. Sandanayake, *Top. Curr. Chem.* **1993**, *168*, 223−264. − [2e] A. P. De Silva, C. P. McCoy, *Chem. Ind.* **1994**, 992−996. − [2f] L. Fabbrizzi, A. Poggi, *Chem. Soc. Rev.* **1995**, *24*, 197−202. − [2g] A. P. de Silva, H. Q. N. Gunaratne, T. Gunnlaugsson, A. J. M. Huxley, C. P. McCoy, J. T. Rademacher, T. E. Rice, *Chem. Rev.* **1997**, *97*, 1515−1566. − [2h] M. D. Ward, *Chem. Ind.* **1997**, 640−645. − [2i] V. Balzani, M. Gopéz-Lopéz, J. F. Stoddart, *Acc. Chem. Res.* **1998**, *31*, 405−414. − [2j] J.-P. Sauvage, *Acc. Chem. Res.* **1998**, *31*, 611−619. − [2k] P. L. Boulas, M. Gomez-Kaifer, L. Echegoyen, *Angew. Chem. Int. Ed.* **1998**, *37*, 216−247. − [2l] A. Niemz, V. M. Rotello, *Acc. Chem. Res.* **1999**, *32*, 42−52. − [2m] A. E. Kaifer, *Acc. Chem. Res.* **1999**, *32*, 62−71. − [2n] D. A. Leigh, A. Murphy, *Chem. Ind.* **1999**, 178−183. − [2o] V. Balzani, A. Credi, F. M. Raymo, J. F. Stoddart, *Angew. Chem. Int. Ed.* **2000**, *39*, 3348−3391.[2p] M. D. Ward, *Chem. Ind.* **2000**, 22−26.

[3] For the first example of a "molecular shuttle", see: P.-L. Anelli, N. Spencer, J. F. Stoddart, *J. Am. Chem. Soc.* **1991**, *113*, 5131−5133.

[4] [4a] R. A. Bissell, E. Córdova, A. E. Kaifer, J. F. Stoddart, *Nature* **1994**, *369*, 133−137. − [4b] M.-V. Martínez-Díaz, N. Spencer, J. F. Stoddart, *Angew. Chem. Int. Ed. Engl.* **1997**, *36*, 1904−1907. − [4c] H. Murakami, A. Kawabuchi, K. Kotoo, M. Kunitake, N. Nakashima, *J. Am. Chem. Soc.* **1997**, *119*, 7605−7606. − [4d] P. R. Ashton, R. Ballardini, V. Balzani, I. Baxter, A. Credi, M. C. T. Fyfe, M. T. Gandolfi, M. Gómez-López, M.-V. Martínez-Díaz, A. Piersanti, N. Spencer, J. F. Stoddart, M. Venturi, A. J. P. White, D. J. Williams, *J. Am. Chem. Soc.* **1998**, *120*, 11932−11942. − [4e] N. Armaroli, V. Balzani, J.-P. Collin, P. Gaviña, J.-P. Sauvage, B. Ventura, *J. Am. Chem. Soc.* **1999**, *121*, 4397−4408. − [4f] J.-P. Collin, P. Gaviña, J.-P. Sauvage, *New J. Chem.* **1999**, *21*, 525−528. − [4g] R. Ballardini, V. Balzani, W. Dehaen, A. Dell′Erba, F. M. Raymo, J. F. Stoddart, M. Venturi, *Eur. J. Org. Chem.* **2000**, 591−602.

[5] [5a] A. Livoreil, C. O. Dietrich-Buchecker, J.-P. Sauvage, *J. Am. Chem. Soc.* **1994**, *116*, 9399−9400. − [5b] P. R. Ashton, R. Ballardini, V. Balzani, M. T. Gandolfi, D. J. F. Marquis, L. Pérez-García, L. Prodi, J. F. Stoddart, M. Venturi, *J. Chem. Soc., Chem. Commun.* **1994**, 177−180. − [5c] M. J. Gunter, M. R. Johnston, *J. Chem. Soc., Chem. Commun.* **1994**, 829−830. − [5d] P. R. Ashton, R. Ballardini, V. Balzani, A. Credi, M. T. Gandolfi, S. Menzer, L. Pérez-García, L. Prodi, J. F. Stoddart, M. Venturi, A. J. P. White, D. J. Williams, *J. Am. Chem. Soc.* **1995**, *117*, 11171−11197. − [5e] D. Cárdenas, A. Livoreil, J.-P. Sauvage, *J. Am. Chem. Soc.* **1996**, *118*, 11980−11981. − [5f] A. Livoreil, J.-P. Sauvage, N. Armaroli, V. Balzani, L. Flamigni, B. Venture, *J. Am. Chem. Soc.* **1997**, *119*, 12114−12124. − [5g] F. Baumann, A. Livoreil, W. Kaim, J.-P. Sauvage, *Chem. Commun.* **1997**, 35−36. − [5h] M. Asakawa, P. R. Ashton, V. Balzani, A. Credi, C. Hamers, G. Mattersteig, M. Montalti, A. N. Shipway, N. Spencer, J. F. Stoddart, M. S. Tolley, M. Venturi, A. J. P. White, D. J. Williams, *Angew. Chem. Int. Ed.* **1998**, *37*, 333−337. − [5i] V. Balzani, A. Credi, S. J. Langford, F. M. Raymo, J. F. Stoddart, M. Venturi, *J. Am. Chem. Soc.* **2000**, *122*, 3542−3543. − [5j] V. Balzani, A. Credi, G. Mattersteig, O. A. Matthews, F. M. Raymo, J. F. Stoddart, M. Venturi, A. J. P. White, D. J. Williams, *J. Org. Chem.* **2000**, *65*, 1924−1936.

[6] [6a] D. Pasini, F. M. Raymo, J. F. Stoddart, *Gazz. Chim. Ital.* **1995**, *125*, 431−435. − [6b] D. B. Amabilino, F. M. Raymo, J. F. Stoddart, *Comprehensive Supramolecular Chemistry*, Vol. 9 (Eds.: M. W. Hosseini, J.-P. Sauvage), Pergamon, Oxford, **1996**, 85−130. − [6c] R. E. Gillard, F. M. Raymo, J. F. Stoddart, *Chem. Eur. J.* **1997**, *3*, 1933−1940. − [6d] F. M. Raymo, J. F. Stoddart, *Chemtracts* **1998**, *11*, 491−511.

[7] For a [2]catenane incorporating two 4,4′-azopyridinium units, see: M. Nakagawa, M. Rikukawa, K. Sanui, N. Ogata, *Supramol. Sci.* **1998**, *5*, 83−87.

[8] The reduction of a 4,4′-azopyridinium unit has been also observed in a dinuclear complex incorporating two $(NH_3)_5Ru^{II}$ groups bridged by a 4,4′-azopyridinium ligand. Upon acidification, an intramolecular redox reaction occurs spontaneously. This process involves the protonation and reduction of the 4,4′-azopyridinium ligand and the concomitant oxidation of the metal centers to afford a dinuclear complex composed of a 4,4′-hydrazopyridinium ligand and two terminal $(NH_3)_5$RuIII groups. J.-P. Launay, M. Tourrel-Pagis, J.-F. Lipskier, V. Marvaud, C. Joachim, *Inorg. Chem.* **1991**, *30*, 1033−1038.

[9] An equimolar CD_3CN solution of host and guest was diluted in twenty steps from 10^{-2} to 10^{-4} M. At each step the solution was left standing for 30 min. at 25 °C and an ^{1}H NMR spectrum was recorded. The chemical shift change ($\Delta\delta_o$) observed for the β-pyridinium protons of the guest was plotted against the concentration (c). The association constant (K_a) and the maximum chemical shift change ($\Delta\delta_m$) were determined by nonlinear curve fitting of this plot using Equation (1). The free energy of association ($\Delta G°$) was calculated using Equation (2) where R and T are the gas constant and the temperature. For equations (1) and (2), see: K. A. Connors, *Binding Constants*, Wiley, New York, **1987**.

$$\Delta\delta_o = \frac{\Delta\delta_m + 2cK_a\Delta\delta_m - \sqrt{\Delta\delta_m{}^2 + 4cK_a\Delta\delta_m{}^2}}{2cK_a} \quad (1)$$

$$\Delta G° = -RT \ln K_a \quad (2)$$

[10] The rate constant (k_c) and the free energy of activation ($\Delta G_c^{\ddagger}$) at the coalescence temperature were calculated using equations (2) and (3), respectively. Δν is the limiting frequency separation and R, k and h are the gas, Boltzmann, and Planck constants,

respectively. For equations (3) and (4), see: I. O. Sutherland, *Annu. Rep. NMR Spectrosc.* **1971**, *4*, 71−235.

$$k_c = \frac{\pi \Delta\nu}{\sqrt{2}} \quad (3)$$

$$\Delta G_c^{\ddagger} = RT_c \ln \frac{kT_c}{hk_c} \quad (4)$$

[11] [11a] P. R. Ashton, R. Ballardini, V. Balzani, M. T. Gandolfi, D. J.-F. Marquis, L. Pérez-García, L. Prodi, J. F. Stoddart, M. Venturi, *J. Chem. Soc., Chem. Commun.* **1994**, 177−180. − [11b] P. R. Ashton, L. Pérez-García, J. F. Stoddart, A. J. P. White, D. J. Williams, *Angew. Chem. Int. Ed. Engl.* **1995**, *34*, 571−574. − [11c] P. R. Ashton, R. Ballardini, S. Menzer, L. Pérez-García, J. F. Stoddart, M. Venturi, A. J. P. White, D. J. Williams, *J. Am. Chem. Soc.* **1995**, *117*, 11171−11197.

[12] [12a] M. Asakawa, M. Higuchi, G. Mattersteig, T. Nakamura, A. R. Pease, F. M. Raymo, T. Shimizu, J. F. Stoddart, *Adv. Mater.* **2000**, *12*, 1099−1102. − [12b] C. P. Collier, G. Mattersteig, E. W. Wong, Y. Luo, K. Beverly, J. Sampaio, F. M. Raymo, J. F. Stoddart, J. R. Heath, *Science* **2000**, *289*, 1172−1175.

[13] B. S. Furniss, A. J. Hannaford, P. W. G. Smith, A. R. Tatchell, *Practical Organic Chemistry*, Longman, New York, **1989**.

[14] P. L. Anelli, P. R. Ashton, R. Ballardini, V. Balzani, M. Delgado, M. T. Gandolfi, T. T. Goodnow, A. E. Kaifer, D. Philp, M. Pietraszkiewicz, L. Prodi, M. V. Reddington, A. M. Z. Slawin, N. Spencer, J. F. Stoddart, C. Vicent, D. J. Williams, *J. Am. Chem. Soc.* **1992**, *114*, 193−218.

[15] P. R. Ashton, E. J. T. Chrystal, J. P. Mathias, K. P. Parry, A. M. Z. Slawin, N. Spencer, J. F. Stoddart, D. J. Williams, *Tetrahedron Lett.* **1987**, *28*, 6367−6370.

[16] P. R. Ashton, R. Ballardini, V. Balzani, M. Belohradsky, M. T. Gandolfi, D. Philp, L. Prodi, F. M. Raymo, M. V. Reddington, N. Spencer, J. F. Stoddart, M. Venturi, D. J. Williams, *J. Am. Chem. Soc.* **1996**, *118*, 4931−4951.

[17] A. Kirpal, E. Rerfer, *Chem. Ber.* **1927**, *60*, 664−666.

Received July 26, 2000
[O00388]